2021 43rd Annual International Conference of the
IEEE Engineering in Medicine & Biology Society (EMBC)
Oct 31 - Nov 4, 2021. Virtual Conference

Estimation of Physiological Impedance from Neuromuscular Pulse Data

Bryan D. Chiles, ASE, *Member IEEE*; Max H. Nerheim, MSEE, *Member IEEE*;
Ryan C. Markle, BSEE, *Member IEEE*; Michael A. Brave, MS, JD, *Sr. Member IEEE*;
Dorin Panescu, PhD, *Fellow IEEE*; Mark W. Kroll, PhD, *Fellow IEEE*

Introduction: A Conducted Electrical Weapon (CEW) deploys 2, or more, probes to conduct current via the body to induce motor-nerve mediated muscle contractions, but the inter-probe resistances can vary and this can affect charge delivery. For this reason, newer generation CEWs such as the TASER® X3, X2 and X26P models have feed-forward control circuits to keep the delivered charge constant regardless of impedance. Our main goal was to explore the load limits for this "charge metering" system. A secondary goal was to evaluate the reliability of the "Pulse Log" stored data to estimate the load resistance.
Methods: We tested 10 units each of the X2 (double shot), X26P, and X26P+ (single-shot) CEW models. We used non-inductive high-voltage resistor assemblies of 50, 200, 400, 600, 1k, 2.5k, 3.5k, 5k, and 10k Ω, a shorted output (nominal 0 Ω), and arcing open-circuits. The Pulse Log data were downloaded to provide the charge value and stimulation and arc voltages for each of the pulses in a 5 s standard discharge cycle.
Results: The average reported raw charge was 65.4 ± 0.2 µC for load resistances < 1 kΩ consistent with specifications for the operation of the feed-forward design. At load resistances ≥ 1 kΩ, the raw charge decreased with increasing load values. Analyses of the Pulse Logs, using a 2-piece multiple regression model, were used to predict all resistances. For the resistance range of 0 – 1 kΩ the average error was 53 Ω; for 1 kΩ – 10 kΩ it was 16%. Muzzle arcing can be detected with a model combining parameter variability and arcing voltage.
Conclusions: The X2, X26P, and X26P+ electrical weapons deliver an average charge of 65 µC with a load resistance < 1 kΩ. For loads ≥ 1 kΩ, the metered charge decreased with increasing loads. The stored pulse-log data for the delivered charge and arc voltage allowed for methodologically-reliable forensic analysis of the load resistance with useful accuracy.

INTRODUCTION

Human electronic control with the Conducted Electrical Weapon (CEW) has gained widespread acceptance as the preferred law enforcement intermediate force option. Presentation compliance is 75 - 85%.[1-3] Subject mortality is reduced by 2/3.[4, 5] Subject injuries, requiring medical attention, are reduced by 80%.[6]

B. Chiles is Sr. Investigations Engineer at Axon Enterprise, Inc. (Axon) (e-mail: bchiles@axon.com).
M. Nerheim is Technical Fellow and Vice President of Research at Axon (e-mail: max@axon.com).
M. Brave is Manager/Member of LAAW International, LLC, and an employee of Axon, and legal advisor to the Axon Scientific and Medical Advisory Board (SMAB) (e-mail: brave@laaw.com).
R. Markle is Sr. Electrical Engineer at Axon. (email: rmarkle@axon.com).
D. Panescu is Chief Technical Officer, Vice President R&D, HeartBeam, Inc. (e-mail: panescu_d@yahoo.com). Dr. Panescu is a paid consultant to Axon.
M. Kroll is Adj. Prof. of Biomedical Engineering at California Polytechnical Univ. (e-mail: mark@kroll.name). Member Axon SMAB & Corporate Board.
All authors have served as expert witnesses for Axon, law enforcement, or in Coroners' Proceedings. Research supported by Axon.

The short-duration electrical pulses applied are intended to stimulate Type A-α motor neurons, which are the nerves that control skeletal muscle contraction, but with minimal risk of stimulating myocardium. This typically leads to a loss of regional muscle control and can result in a fall to the ground to end a potentially violent confrontation or suicide attempt.[7-9] The X2 and X26P models deliver the pulses (shown in Figure 1) at an average rate of 19.6 pulses-per-second (PPS). (X2/X26P firmware before October 2016 controlled pulse delivery at 19 PPS).

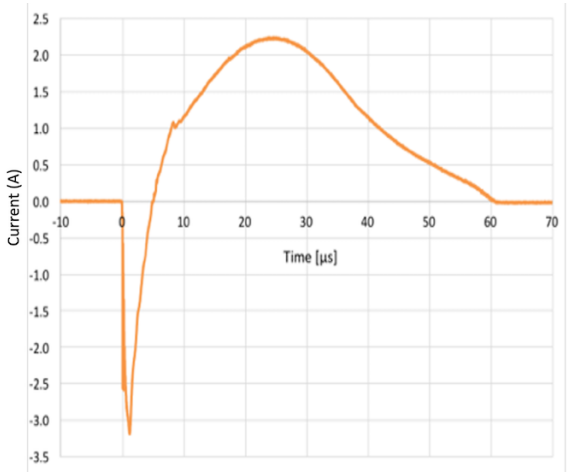

Figure 1. Typical X2 and X26P waveform.

A CEW deploys 2, or more, probes using inert compressed gas. To gain probe separation, the top probe deploys generally straight to the target, while the bottom probe deploys at a 7 or 8° downward angle. The resistance R between cylindrical darts of length L, diameter d, in a semi-infinite medium of bulk resistivity ρ is given by Equation 1. This assumes that D (the spacing between the darts) is < 8L i.e., in the near-field region:[10]

Equation 1 $$Z = \frac{\rho ln[D/d]}{\pi L}$$

If the probes are further apart, with a spacing distance D > 8L, in a semi-infinite medium, then there are no material near-field effects and the resistance is given by Equation 2. Note that the resistance is constant with respect to probe spacing.

Equation 2 $$Z = \frac{\rho ln[4L/d]}{\pi L}$$

Fully-inserted probe darts reside in a multi-layered region of tissue beginning with skin (ρ=5 kΩ•cm), fat (2500 Ω•cm), and

skeletal muscle (220 Ω•cm along fiber orientation).[11, 12] For adults of typical body habitus, a melded resistivity value of 600 Ω•cm provides good estimations of inter-probe resistance. For a typical CEW probe *fully-inserted* dart of length 1.2 cm, diameter 0.08 cm and a resistivity of 600 Ω•cm, the calculated resistance is 570 Ω. This value is close to the measured human inter-probe resistance for 12 mm darts spaced 25 cm apart.[13]

With a probe spacing of > 25 cm, the influence of the skeletal muscle begins to dominate (due to the deeper current lines) and the inter-probe resistance paradoxically begins to decrease with increasing spacing as shown in Figure 2.[13] Those results are from human testing with probes in the front chest and abdomen so the increased probe spacing may have allowed for currents around the back to lower the net resistance. Additionally, overall average electrical resistivity might have been affected by a greater variety of tissues present between the probes.

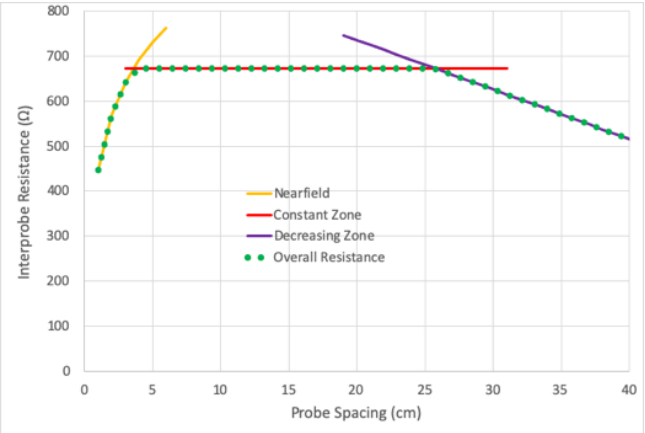

Figure 2. Typical values of resistance as a function of probe spread for fully-inserted 12 mm shafts.

The exemplar CEW pulse shown in Figure 1 used a 600 Ω load. By convention, the "main" phase is defined as being positive and delivers the vast majority of the charge. The initial brief negative-phase serves to establish an electric arc, creating a conductive path to bridge an air gap when there is no galvanic connection. With bulky or baggy clothing, a CEW probe may fail to initiate or maintain direct skin contact and thus arcing is required to complete the circuit.[14, 15] The completion of the conductive path by the arc allows the lower-voltage main-phase current to then flow thru the circuit. The duration of the pulse is defined as the time from the 1st downward transition below -100 mA (-60 V with the 600 Ω load) up until the last downward transition below a value of +100 mA (60 V) according to the ANSI (American National Standards Institute) CPLSO-17 (2017) standard.[16] The "raw charge" is the integrated value across the full duration of the pulse. Note that the raw charge is always *less* than that of the main phase since the arc phase contributes a *negative* charge, thus cancelling some of the main phase charge. Since the arc-phase charge is about 5 µC, the main-phase charge value equals the raw-charge plus 5 µC.

The inter-probe resistance can vary significantly, and this can affect charge delivery. The ANSI CPLSO-17 standard requires (among other things) that the charge be between a minimum of 40 µC (for incapacitation performance) and a maximum of 125 µC (for cardiac safety). The load impedance can be high when the cartridge probes connect by arcing to skin, or with a probe's dart in a high adipose fat location of the body. The load impedance can be low when the probes are across metal, such as a belt buckle. The load impedance is optimal when both probes are penetrating the skin and discharging into the less resistive soft tissue. Further, the load resistance can vary from low to high rapidly during the activation cycle if the probe is moving.

Modern TASER® brand CEWs record information in the "Trilogy" Logs: Event, Engineering, and Pulse logs. The "Event" logs give the times and durations of all trigger activations, arc switch activations (X2 only), along with transitions of the safety switch, USB connections, time synchronizations, and firmware updates.[17] The "Engineering" logs provide diagnostic information for troubleshooting. The Event and Engineering logs are not relevant to the topics in this paper and will not be discussed further.

The Pulse-Log memory includes the pulse-by-pulse voltage stored on the arc and stimulation capacitors and the measured charge. The arc voltage is the voltage across the arc capacitors driving the primary of the output transformer, as shown in Figure 3. This voltage shows what level the capacitors needed to be in order to generate an output pulse. The stim voltage is the voltage across the stimulation capacitor which is dumped directly into the output connections in series with the transformer secondary and shows what level the capacitors needed to be in order to produce the electrical output charge measured.

Once the trigger is pulled, the microcontroller (U1) begins to charge the arc and stimulation capacitors by switching the Q1 MOSFET off and on. While charging, the microcontroller is constantly monitoring the voltage on these capacitors through their respective voltage dividers until their target voltage levels have been reached: 800 V and 2400 V for the first charge cycle, respectively. At this point, charging of the output capacitors is discontinued and generation of an output pulse is attempted by firing the SCR (Q2). Once enabled, current flows from the arc capacitor thru the primary windings of the output transformer (T2). This induces energy into the secondary windings, causing the voltage potential on the secondary windings to rise until a level is reached that can ionize the arc gap between the device and the intended load. Once ionization of the output arc gap is achieved and the energy from the arc capacitor has been depleted, current will flow from the stimulation capacitors through the secondary windings, load, and charge sense capacitor. During discharge of the stimulation capacitors, energy is again stored in the secondary windings of the output transformer. Once the energy is depleted from the stimulation capacitors, the stored energy in the secondary windings will be discharged through the load – completing delivery of the output pulse to the load. After the pulse has been generated, the microcontroller samples the voltage on the charge sense capacitor and calculates Q = CV. Based on this result, the microcontroller adjusts the voltage levels of the arc and stimulation capacitors

as necessary until the target charge level of 65 µC is achieved on the subsequent pulses. The microcontroller will repeat this process 19.6 times per second for each active cartridge bay.

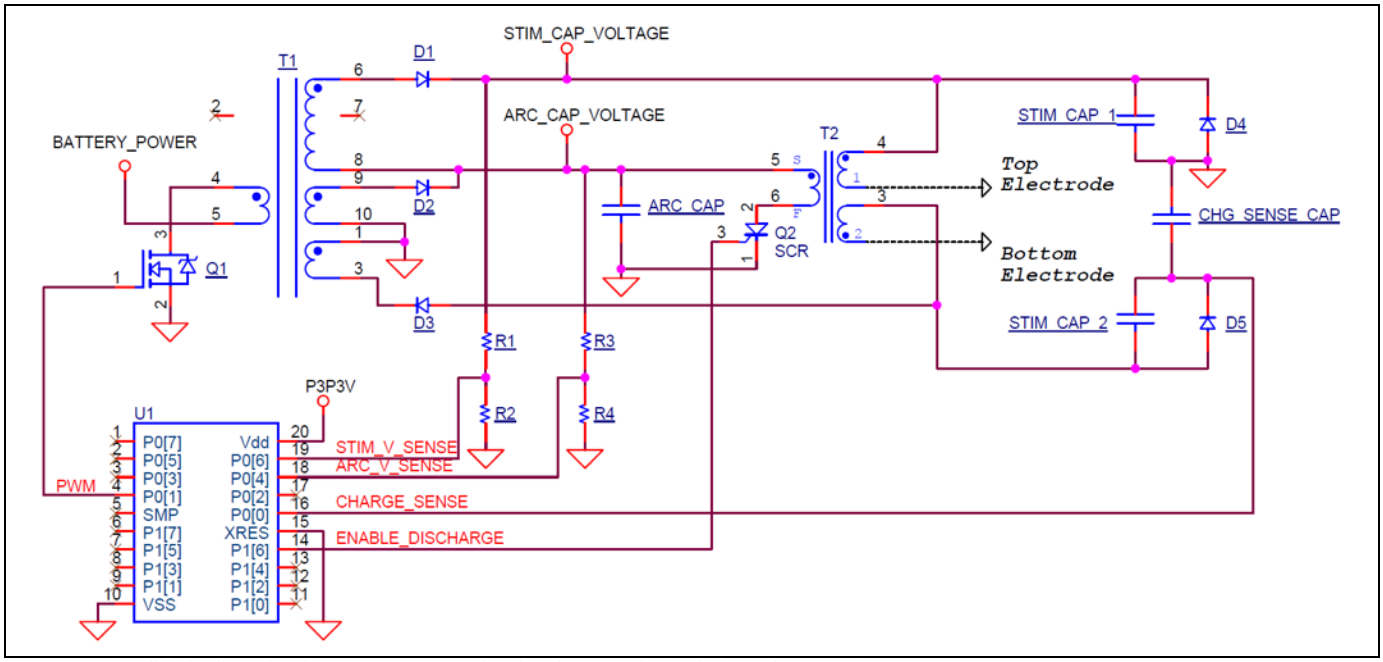

Figure 3. Simplified schematic of CEW output stage showing the arc and stimulation voltage sensing.

The "Charge Metering" described above regulates the raw output charge to a target level typically 63–65 µC depending on the model. (Note that this implies a main-phase charge of 68–70 µC.) When the CEW trigger is first pulled, it charges the arc and stimulation capacitors to a nominal voltage. If the measured charge is significantly different than the target value, the charge-voltages of the arc and stim capacitors are adjusted by 2 A/D converter counts, approximately 42 and 127 V, for the stimulation and arc capacitor respectively, before the next pulse.

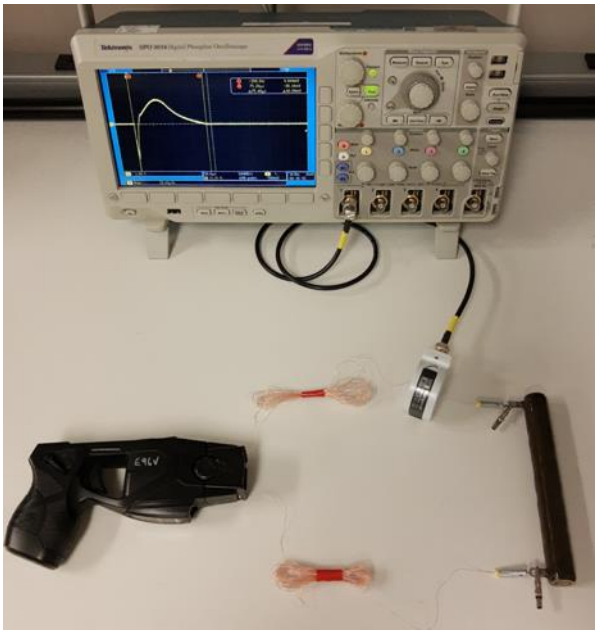
Figure 4. X26P test setup.

When the delivered charge is closer to the target value the charge voltages of the arc and stimulation capacitors are adjusted by 1 ADC count (approximately 21 and 64 V for stimulation and arc capacitors respectively). The charge is measured again on the next pulse and the voltage is again adjusted accordingly. For extreme load values, stability of the charge obtains in about 200–400 ms. If the load impedance is very high (> 1 kΩ), resulting in a low charge, the arc and stim voltages are increased up to a threshold value where they reach the maximum voltage allowed for the capacitors. Once the capacitors are at their maximum permitted voltage, the delivered charge will not increase further, unless the load impedance drops. If the load impedance drops and the charge increases *above* the target value, the CEW will lower the voltage on the arc and stim capacitors until the charge drops to the target value.

The primary goal of this study was to explore the load limits where the charge metering feedback system can maintain the charge at the target level even with partially inserted probes or with probes lodged in clothing and connected only via arcing which can lead to resistances of several kΩ. The secondary goal was to evaluate the reliability of the Pulse Log stored data to reasonably estimate the load resistance value and to diagnose open-circuit muzzle arcing.

METHODS:

We tested 10 units each of the X2 (double cartridge) model and 10 units of the X26P and X26P+ (single cartridge) models. Note: the "X26P+" is a designation of convenience for the X26P using a cartridge with an internal arc gap of 8.0 mm vs. the previous gap of 1.3 mm. We used non-inductive high-voltage resistor assemblies of 50, 200, 400, 600, 1k, 1.5k, 2.5k, 3.5k, 5k, 10 kΩ, a shorted output (nominal 0 Ω), and

various open-circuits (to cause arcing across the CEW muzzle). A Stangenese "0.5-1.0 W" model high-frequency 0.5% accuracy current transformer was used to monitor the outputs to verify operation of the CEW as shown in Figure 4.

The Pulse Log data were downloaded to provide the charge and the stimulation and arc voltages for each of the pulses in a single 5 s standard delivery cycle. See Figure 5.

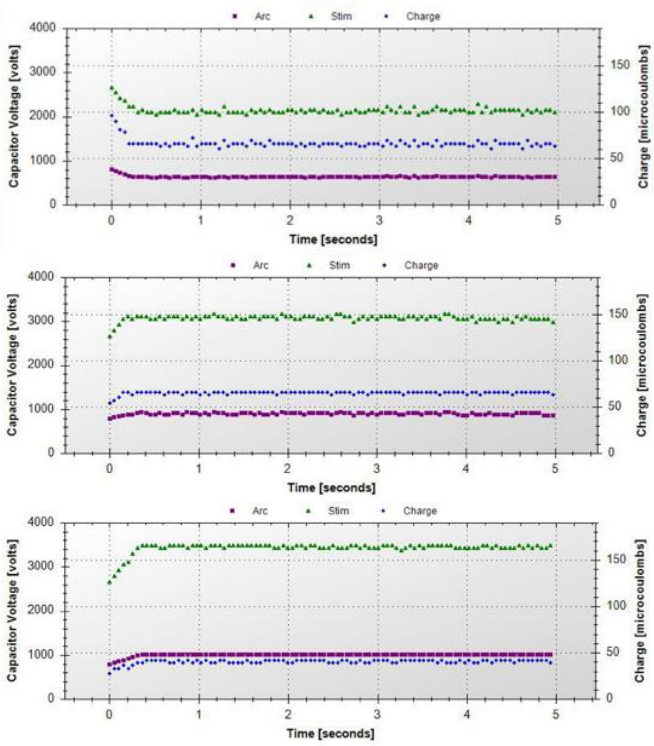

Figure 5. Pulse logs from X2 for 0 Ω, 600 Ω, and 5k Ω loads (top to bottom).

Note that the capacitor charge voltages were adjusting down initially for the 0 Ω load while adjusting up for the 600 Ω and 5 kΩ loads. To allow for the charge-metering adjustments, the initial 1 second was ignored and only the last 4 seconds (≈ 78 pulses) were analyzed. These were averaged to produce a charge value along with arc- and stim- voltages for each load and unit. The standard deviations of these values were also calculated over the 4 s period.

RESULTS:

The arc voltage increased monotonically from 600 V to ≈ 1 kV over the resistance range of 0-1 kΩ as seen in Figure 6. The arc voltage stayed relatively constant at load values over 1 kΩ. This suggested that the arc voltage is a useful predictor of the load resistance only for R ≤ 1 kΩ.

As shown in Figure 7, the reported average charge was extremely consistent at 65.37 ± 0.20 µC for the load resistances < 1 kΩ, consistent with the operation of the feedback design. Due to the tolerances of the sense and measurement circuitry and components within the X2 CEW, this reported charge is slightly higher than the actual delivered charge of 63.5 ± 1.8 µC as measured by external instrumentation.[18]

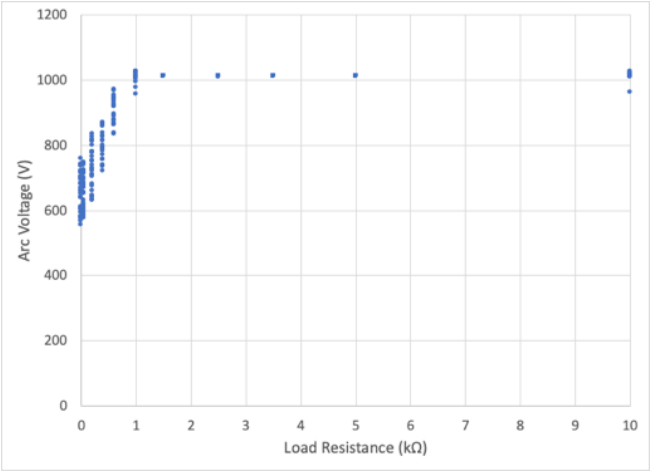

Figure 6. Arc voltage as function of the load resistance.

For loads ≥ 1 kΩ, the metered charge decayed in a semi-hyperbolic manner suggesting that the charge would be a useful predictor of the conductance (reciprocal of the resistance) for charges < 60 µC.

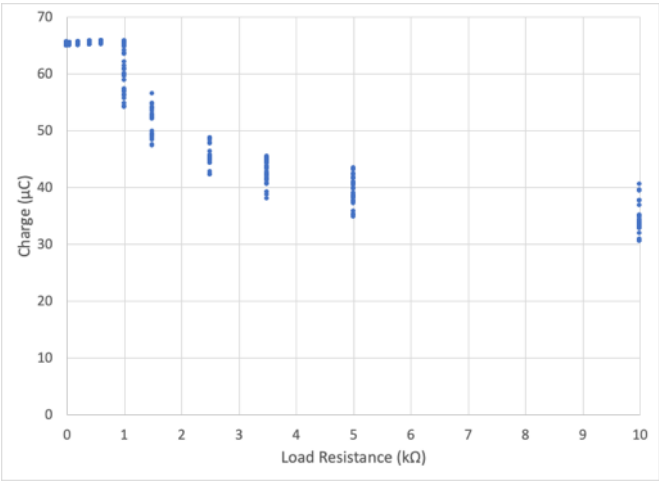

Figure 7. Charge delivered as a function of load resistance.

RESISTANCE MODELING

JMP v14.0 was used for statistical analysis. For the resistance modeling, the samples of muzzle arcing were excluded. Attempts were made to predict the load resistance with an omnibus multiple-regression model, but this proved impractical. This was not surprising given the sharp inflection point at 1 kΩ (load resistance) and 60 µC (delivered charge). We then fit the data with a 2-piece model bifurcated at Q = 60 µC.

For Q ≥ 60 µC the prediction model was:

Equation 3 $$R = 4.94[V_{arc}/Q]^2 + 9.3\sqrt{V_{stim}} - 908\ \Omega$$

Where V_{arc} and V_{stim} are the arcing and stim voltage (V) and Q is the charge (µC). Note that V_{arc}/Q is an Ohm's law analog for the resistance. The formula has a slight modification (+ 3.88Q) for the short-gap X26P:

Equation 4 $R = 4.94[V_{arc}/Q]^2 + 9.3\sqrt{V_{stim}} - 908\ \Omega + 3.88Q$

This overall model had $r^2 = 0.97$. The RMS prediction error was 57.5 Ω.

For Q < 60 µC, the best models (for R) were complex with large RMS errors which we judged inadequate. We then modeled the root-conductance ($1/\sqrt{R}$) based on the semi-hyperbolic plot seen in Figure 7.

A surprisingly efficient model was:

Equation 5 $1/\sqrt{R} = 0.0003Q^2 - 0.00933$ [R in kΩ]

This had $r^2 = 0.91$. After squaring and inverting, the average error was 16% over the range of 1-10 kΩ.

Based on the consolidated model, these CEW models satisfy the ANSI raw-charge minimum value of 40 µC for loads up to 10 kΩ. The average charges were ≤ 65.6 µC. There was no violation of the ANSI upper limit of 125 µC.

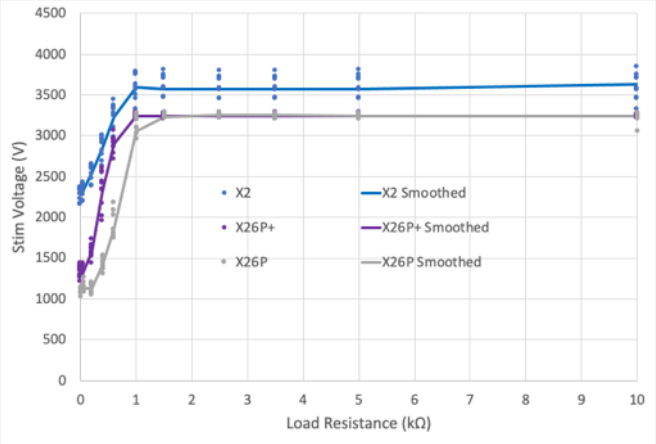

Figure 8. Stimulation voltage as function of load resistance.

The stimulation voltage was reliable as a predictor in the Q ≥ 60 µC zone, primarily because it had dependence on the CEW model (X2 or X26P/+) as shown in Figure 8.

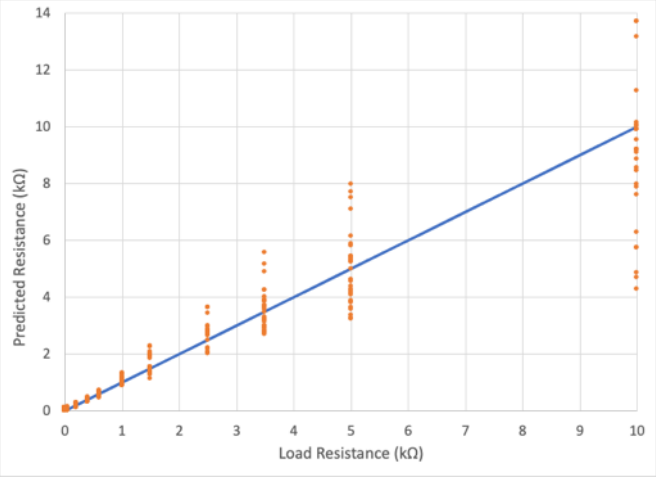

Figure 9. Predicted vs actual resistance.

The overall 2-piece model performance is shown in Figure 9. (Negative value predictions were set to 0 Ω.) For the range of 1-10 kΩ the average error was 16%. For the resistance range of 0-1 kΩ a percentage error cannot be calculated; the average error was 52.6 Ω.

When the load resistance is ≥ 1 kΩ, the circuitry runs open-loop and thus the variability of the charge and hence the resistance predictions increase significantly. However, for the physiological loads, which are < 1 kΩ, the predictive accuracy is quite good.

MUZZLE ARCING

With an open circuit — from a detached or broken wire or dislodged probe — the CEW will arc across the muzzle (see Figure 10) and output a full normal charge (on average).

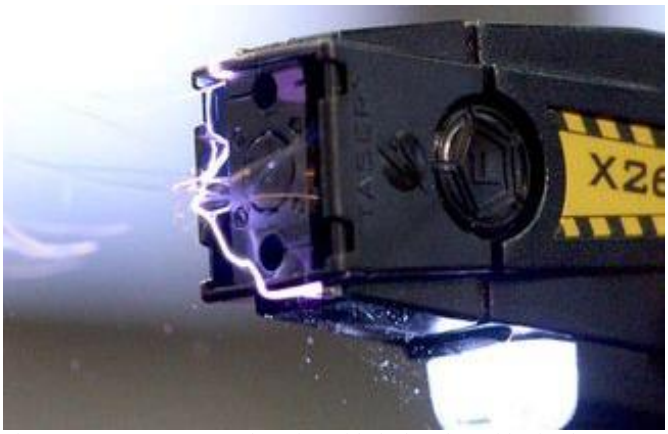

Figure 10. X26P CEW muzzle arcing with deployed cartridge in place

In addition, the recorded parameters are consistent with typical load resistances and thus the above prediction models would give misleading load estimates. However, the instability of the arc increases the standard deviation of the charge as seen in Figure 11 and this can be reliably used as a predictor.

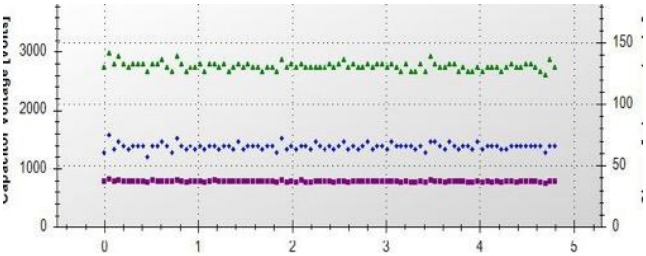

Figure 11. Pulse graph for X2 muzzle arcing across undeployed cartridges.

A discriminant function was calculated using a quadratic (differing covariance) model to differentiate open circuit arcing from a resistive load where R < 5 kΩ and where σ is the standard deviation:

Equation 6 $D = 1.304\ \sigma(Q) + 2.825\sqrt{V_{arc}} - 0.02\ \sigma(V_{stim}) - 0.0000281V_{arc}^2$

For D > 64 arcing is predicted with an accuracy of > 99%; for D < 62.5, the presence of a resistive load is predicted with an accuracy of > 95%.

Arcing can occur across either the muzzle or the distal cartridge end if one is installed. For muzzle arcing, V_{arc} = 972 ± 58 V vs. 828 ± 43 V for a cartridge arc and thus a voltage boundary of 900 V can be used to separate those conditions.

LIMITATIONS

The Pulse Logs can provide reliable and consistent evidence of a charge delivered into a load. They do not provide any evidence of the nature of the load (human, animal, water, or other). Thus, they are a synergistic element of the objective evidence, to be combined with other objective evidence, to conclude whether the pulse was delivered into a person or not. The Pulse Logs also give no indication of incapacitation performance as that is significantly dependent on probe spread and locations and other factors on the body.[7, 9]

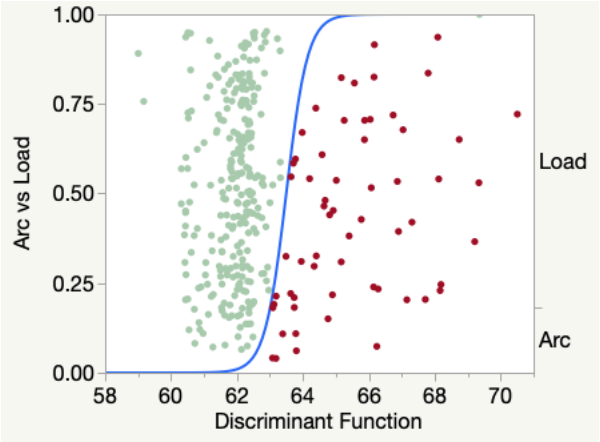

Figure 12. Arc prediction from discriminant function.

CONCLUSIONS

The tested X2 and X26P electrical weapons reported an average raw charge of 65 µC with a load resistance of < 1 kΩ. For loads ≥ 1 kΩ, the metered charge decreased with increasing loads. The stored pulse-log data for the delivered charge and arc voltage allowed for objective methodologically-reliable forensic analysis of the load resistance. The presence of arcing can be diagnosed using the pulse-log data and the variability of the charge and stimulation voltage.

REFERENCES

[1] R. Stevenson and I. Drummond-Smith, "Medical implications of Conducted Energy Devices in law enforcement," *Journal of Forensic and Legal Medicine,* p. 101948, 2020.

[2] N. Grove, C. Grove, O. Peschel, and S. Kunz, "Welfare effects of substituting traditional police ballistic weapons with non-lethal alternatives: Medico-economic comparative study," *Rechtsmedizin,* vol. 26, no. 5, pp. 418-424, 2016, doi: 10.1007/s00194-016-0117-y.

[3] G. den Heyer, "An analysis of the effectiveness and use by the New Zealand Police of the TASER from 2009 to 2017," *International Journal of Police Science & Management,* vol. 22, no. 4, pp. 356-365, 2020.

[4] F. V. Ferdik, R. J. Kaminski, M. D. Cooney, and E. L. Sevigny, "The Influence of Agency Policies on Conducted Energy Device Use and Police Use of Lethal Force," *Police Quarterly,* p. 1098611114548098, 2014.

[5] M. Kroll, M. Brave, H. Pratt, K. Witte, S. Kunz, and R. Luceri, "Benefits, Risks, and Myths of TASER® Handheld Electrical Weapons," *Human Factors and Mechanical Engineering for Defense and Safety,* vol. 3, no. 1, p. 7, 2019.

[6] B. Taylor and D. J. Woods, "Injuries to officers and suspects in police use-of-force cases: A quasi-experimental evaluation," *Police Quarterly,* vol. 13, no. 3, pp. 260-289, 2010.

[7] J. Ho, D. Dawes, J. Miner, S. Kunz, R. Nelson, and J. Sweeney, "Conducted electrical weapon incapacitation during a goal-directed task as a function of probe spread," *Forensic Sci Med Pathol,* vol. 8, no. 4, pp. 358-66, Dec 2012, doi: 10.1007/s12024-012-9346-x.

[8] J. C. Criscione and M. W. Kroll, "Incapacitation recovery times from a conductive electrical weapon exposure," *Forensic Sci Med Pathol,* vol. 10, no. 2, pp. 203-7, Jun 2014, doi: 10.1007/s12024-014-9551-x.

[9] J. Ho *et al.*, "A comparative study of conducted electrical weapon incapacitation during a goal-directed task," *Forensic Sci Med Pathol,* vol. 16, no. 4, pp. 613-621, Dec 2020, doi: 10.1007/s12024-020-00284-7.

[10] S. Grimnes and O. Martinsen, *Bioimpedance and Bioelectricity Basics (3rd ed)*. San Diego: Academic Press, 2015.

[11] S. Rush, J. A. Abildskov, and McFeer, "Resistivity of body tissues at low frequencies," *Circ Res,* vol. 12, pp. 40-50, Jan 1963.

[12] T. J. Faes, H. A. van der Meij, J. C. de Munck, and R. M. Heethaar, "The electric resistivity of human tissues (100 Hz-10 MHz): a meta-analysis of review studies," *Physiol Meas,* vol. 20, no. 4, pp. R1-10, Nov 1999.

[13] D. M. Dawes, J. D. Ho, M. W. Kroll, and J. R. Miner, "Electrical characteristics of an electronic control device under a physiologic load: a brief report," *Pacing Clin Electrophysiol,* vol. 33, no. 3, pp. 330-6, Mar 2010.

[14] A. Adler, "Toward a Test Protocol for Conducted Energy Weapons," *Modern Instrumentation,* vol. 02, no. 01, pp. 7-15, 2013, doi: 10.4236/mi.2013.21002.

[15] C. Mesloh, M. Henych, and R. Wolf, "Less Lethal Weapon Effectiveness, Use of Force, and Suspect & Officer Injuries: A Five-Year Analysis," *Report to the National Institute of Justice,* vol. 224081, pp. 1-103, Sept 2008. [Online]. Available: https://www.ncjrs.gov/pdffiles1/nij/grants/224081.pdf.

[16] ANSI, "Electrical Characteristics of ECDs and CEWs," *American National Standards Institute,* vol. 17, pp. https://estandards.net/product/ansi-cplso-17-2017/, 2017, doi: https://estandards.net/product/ansi-cplso-17-2017/.

[17] M. Kroll, "Baseball, Poison, and Soup Recipes: The TASER Trio of Popular Myths," *ResearchGate.net,* Technical Report pp. 1-3, 2015, doi: 10.13140/RG.2.1.3348.4320.

[18] B. D. Chiles, M. H. Nerheim, M. A. Brave, D. Panescu, and M. W. Kroll, "Electrical Weapon Charge Delivery With Arcing," *Conf Proc IEEE Eng Med Biol Soc,* vol. 2018, pp. 2234-2239, Jul 2018, doi: 10.1109/EMBC.2018.8512753.